

# Hydrogen Bond Network in the Metal Binding Site of Carbonic Anhydrase Enhances Zinc Affinity and Catalytic Efficiency<sup>†</sup>

Laura L. Kiefer, Steven A. Paterno, and Carol A. Fierke\*

Contribution from the Biochemistry Department, Box 3711, Duke University Medical Center, Durham, North Carolina 27710

Received January 24, 1995<sup>⊗</sup>

**Abstract:** In metalloenzymes the side chains that ligand the metal ion are nested in a hydrogen bonding network with other protein residues. In carbonic anhydrase II (CAII) the four zinc ligands, H94, H96, H119, and water, donate hydrogen bonds to the carboxamide of Q92, the backbone carbonyl oxygen of N244, a carboxylate oxygen of E117, and the hydroxyl of T199, respectively. To investigate the functional role of these hydrogen bonds, we determined the effects of varying the structure of the side chain at positions 92, 117, and 199 on zinc binding and catalysis. These functional changes are further illuminated by the X-ray crystal structures of these variants (following paper by Lesburg and Christianson). The data demonstrate that zinc affinity is increased by a factor of 10 per hydrogen bond, presumably by decreasing the entropic cost of zinc binding. The observed decrease in zinc affinity is additive for the Q92A/E117A CAII variant suggesting a maximal decrease of 10<sup>4</sup>-fold for removal of all four hydrogen bonds. Furthermore, the hydrogen bond between H119 and E117 determines slow zinc dissociation. Finally, this hydrogen bond network “fine-tunes” the catalytic efficiency and the zinc–water pK<sub>a</sub> of CAII by modulating the electrostatic environment of the zinc. The resulting negative Brønsted correlation indicates that electrostatic stabilization of both the transition state and hydroxide ion by zinc is the main determinant of catalytic efficiency in CAII. Therefore, indirect ligands are an essential feature of metalloenzymes and should be included in the structure-assisted design of metal binding sites in order to obtain high affinity and reactivity.

## Introduction

A current goal of protein engineering is to design and construct novel metal binding proteins with predictable structure and function. A step toward this goal has been the design of metal sites into a variety of protein scaffoldings (for recent examples see refs 1–7). However, none of these sites possess the avid metal binding and catalytic activity of metalloenzymes observed in nature.<sup>8</sup> The engineered metal sites were designed using mainly the ligand geometry and stereochemistry of structurally-characterized metalloenzymes. Yet, the structure and chemical composition of the surrounding active site cavity in metalloenzymes, including a hydrogen bond network,<sup>9–11</sup> also likely modulate the properties of the metal binding site. Hydrogen bonding interactions with metal ligands are proposed to orient the ligands for optimal metal coordination, enhance

the electrostatic interaction between the ligands and metal ion,<sup>12</sup> and modulate the pK<sub>a</sub> and reactivity of the zinc-bound solvent molecule.<sup>9,10</sup> Carboxylate–histidine–metal interactions have previously been implicated in zinc binding in copper/zinc superoxide dismutase,<sup>13</sup> hydrolytic activity in neutral endopeptidase,<sup>14</sup> and the redox properties of cytochrome *c* peroxidase.<sup>15</sup> However, there is a paucity of detailed structure–function analysis of these important hydrogen bonding networks.

To aid in the design of improved metal binding sites, we are dissecting the essential structural features of the metal binding site of the prototypical zinc enzyme, carbonic anhydrase II (CAII). The physiological function of CAII (EC 4.2.1.1) is the reversible hydration of CO<sub>2</sub> to HCO<sub>3</sub><sup>−</sup> and a proton that occurs with a second-order rate constant approaching the diffusion-control limit.<sup>8,16,17</sup> The three-dimensional structure of this enzyme has been determined<sup>18</sup> and refined at 1.54 Å resolution.<sup>19</sup> The zinc cofactor lies at the bottom of the active site cleft where it is coordinated to H94, H96, H119, and a solvent molecule in a tetrahedral geometry (Figure 1). The protonated nitrogen atoms in the imidazole rings of H94, H96, and H119 donate a hydrogen bond to the carboxamide side chain of Q92, the backbone carbonyl oxygen of N244, and one of the carboxylate oxygens of E117, respectively. (These hydrogen-bonded residues are referred to as “indirect ligands”<sup>9</sup>) The side chain

\* Author to whom correspondence should be addressed.

<sup>†</sup> Abbreviations: CAII, human carbonic anhydrase II; Tris, tris(hydroxymethyl)aminomethane; TAPS, 3-[[tris(hydroxymethyl)methyl]amino]propanesulfonic acid; MOPS, 3-(*N*-morpholino)propanesulfonic acid; MES, 2-(*N*-morpholino)ethanesulfonic acid; EDTA, (ethylenedinitrilo)tetraacetic acid; PAR, 4-(2-pyridylazo)resorcinol; PNPA *p*-nitrophenol acetate.

<sup>⊗</sup> Abstract published in *Advance ACS Abstracts*, June 15, 1995.

(1) Regan, L.; Clark, N. D. *Biochemistry* **1990**, *29*, 10878–10883.

(2) Hellinga, H. W.; Caradonna, J. P.; Richards, F. M. *J. Mol. Biol.* **1991**, *222*, 787–803.

(3) Pessi, A.; Bianchi, E.; Cramer, A.; Venturini, S.; Tramontano, A.; Sollazzo, M. *Nature* **1993**, *362*, 367–369.

(4) Wade, W. S.; Koh, J. S.; Han, N.; Hoekstra, D. M.; Lerner, R. A. *J. Am. Chem. Soc.* **1993**, *115*, 4449–4456.

(5) Stewart, J. D.; Roberts, V. A.; Crowder, M. W.; Getzoff, E. D.; Benkovic, S. J. *J. Am. Chem. Soc.* **1994**, *116*, 415–416.

(6) Handel, T. M.; Williams, S. A.; DeGrado, W. F. *Science* **1993**, *261*, 879–885.

(7) McGrath, M. E.; Haymore, B. L.; Summers, N. L.; Craik, C. S.; Fletterick, R. J. *Biochemistry* **1993**, *32*, 1914–1919.

(8) Christianson, D. W. *Adv. Protein Chem.* **1991**, *42*, 281–355.

(9) Christianson, D. W.; Alexander, R. S. *J. Am. Chem. Soc.* **1989**, *111*, 6412–6419.

(10) Christianson, D. W.; Alexander, R. S. *Nature* **1990**, *346*, 225.

(11) Chakrabarti, P. *Protein Eng.* **1990**, *4*, 57–63.

(12) Argos, P.; Garauito, R. M.; Eventoff, W.; Rossmann, M. G.; Branden, C. I. *J. Mol. Biol.* **1978**, *126*, 141–158.

(13) Banci, L.; Bertini, I.; Cabelli, D. E.; Hallewell, R. A.; Tung, J. W.; Viezzoli, M. S. *Eur. J. Biochem.* **1991**, *196*, 123–128.

(14) Le Moual, H.; Dion, H.; Roques, B. P.; Crine, P.; Boileau, G. *Eur. J. Biochem.* **1994**, *221*, 475–480.

(15) Goodin, D. B.; McRee, D. E. *Biochemistry* **1993**, *32*, 3313–3324.

(16) Silverman, D. N.; Lindsog, S. *Acc. Chem. Res.* **1988**, *21*, 30–36.

(17) Lindsog, S.; Liljas, A. *Curr. Op. Struct. Biol.* **1993**, *3*, 915–920.

(18) Liljas, A.; Kannan, K. K.; Bergsten, P.-C.; Waara, I.; Fridborg, K.; Strandberg, B.; Carlbom, U.; Jarup, L.; Lovgren, S.; Petef, M. *Nature (London), New Biol.* **1982**, *235*, 131–137.

(19) Håkansson, K.; Carlsson, M.; Svensson, L. A.; Liljas, A. *J. Mol. Biol.* **1992**, *227*, 1192–1204.

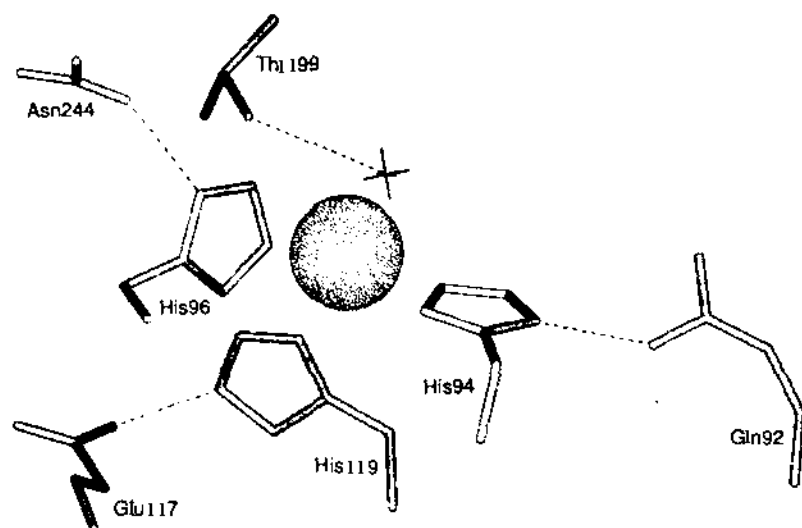


**Figure 1.** Structure of the active site of wild-type CAII taken from the crystal structure of Alexander *et al.*,<sup>54</sup> showing the zinc tetrahedrally coordinated to H94, H96, H119, and a solvent molecule and the residues that hydrogen bond with the zinc ligands. H94, H119, and the zinc-solvent donate a hydrogen bond to the side chains of Q92, E117, and T199, respectively, and H96 donates a hydrogen bond to the backbone carbonyl oxygen of N244.

hydroxyl group of T199 accepts a hydrogen bond from the zinc-bound hydroxide ion and donates a hydrogen bond to E106. This zinc coordination polyhedron is optimized to provide catalytically active zinc-hydroxide at neutral pH.<sup>20–24</sup> CAII-catalyzed hydration proceeds through direct nucleophilic attack of the zinc-bound hydroxide ion on the carbonyl carbon of CO<sub>2</sub> to form a zinc-bound bicarbonate intermediate followed by product dissociation, resulting in the zinc-H<sub>2</sub>O form.<sup>16,25,26</sup>

We are currently delineating the functional importance of the hydrogen bond network of the zinc ligands by characterizing the zinc affinity and catalytic efficiency of a series of CAII variants in the indirect zinc ligands, including Q92 (Q92A, Q92L, Q92N, and Q92E), E117 (E117A, E117D), and T199 (T199A) (see also refs 20–22). These data, in light of structures of many of these variants determined by Lesburg and Christianson,<sup>27</sup> demonstrate that the indirect ligands optimize the catalytic efficiency of CAII and fine-tune the zinc-water pK<sub>a</sub>. However, the major significance of the hydrogen bonds to zinc ligands in CAII is the increased zinc affinity and slow zinc dissociation; about 1.4 kcal/mol of zinc binding energy is conferred per hydrogen bond for up to a 5 kcal/mol increase in zinc affinity for four hydrogen bonds.

## Material and Methods

**Preparation of CAII Variants.** The CAII variants were produced using oligonucleotide-directed mutagenesis of the cloned human CAII gene in pCAM<sup>28</sup> and the entire CAII gene of the variants was sequenced.<sup>29</sup> The plasmids encoding the variant CAII's were transformed into the *E. coli* strain BL21(DE3), and cell growth and protein induction were performed as described previously.<sup>31</sup> The proteins were purified to ≥95% homogeneity either by sequential chromatography

on DEAE-Sephacel and S-Sepharose resins (Q92A, Q92N, E117A, E117D, Q92A/E117A)<sup>31</sup> or by sequential affinity and ion exchange chromatography on sulfonamide<sup>31</sup> and S-Sepharose resins, respectively (Q92L, Q92E, T199A).

**Zinc Analyses, Dissociation Constant, and Dissociation Rate Constant.** All solutions were prepared in plasticware using deionized water (18 MΩ). Apo-CAII's were prepared using Amicon diaflow filtration<sup>32</sup> against first 50 mM dipicolinate, pH 7.0 (0.65 mL/min, 100 min), and then 10 mM Tris sulfate, pH 7.0, followed by chromatography on a PD-10 column (Sephadex G-25M, 5 cm × 15 cm, Pharmacia) equilibrated with 15 mM phosphate buffer, pH 7. Dissociation constants for zinc were obtained by dialyzing apoenzyme for 20 h at 30 °C against a zinc/dipicolinate buffer (0–0.5 mM total zinc/1 mM dipicolinate or 0–0.14 mM total zinc/0.2 mM dipicolinate) in 10 mM Tris sulfate, pH 7; removing unbound zinc by chromatography on a PD-10 column; and quantitating the bound zinc concentration, [E-Zn], with 4-(2-pyridylazo)resorcinol (PAR).<sup>21,31</sup> The concentration of free zinc ([Zn]<sub>free</sub>) in the dialysis buffer was calculated from the dipicolinate-zinc stability constants.<sup>34</sup> The dissociation constant was calculated using the KaleidaGraph (Synergy Software) curve-fitting program with eq 1, where C ranged from 0.9 to 1.3.

$$[E-Zn]/[E]_{tot} = C/(1 + K_D/[Zn]_{free}) \quad (1)$$

The rate constant for zinc dissociation was determined by diluting CAII into 10 mM Tris sulfate, pH 7.0, containing EDTA (final concentration 40–50 μM CAII, 34 mM EDTA) to trap zinc dissociating from the enzyme. At various times after dilution, free zinc and EDTA were removed by PD-10 chromatography and [E-Zn] was quantitated using the PAR assay.<sup>21,33</sup> The total time after dilution was calculated as the sum of the incubation time and the time to complete the PD-10 column (4 min). The dissociation rate constant, zero-point (A<sub>0</sub>) ranged from 0.74 to 1.0, and standard error were calculated using the curve-fitting program KaleidaGraph with eq 2.

$$[E-Zn]/[E]_{tot} = A_0 e^{(-k_1 t)} \quad (2)$$

**Catalytic Activity.** The  $k_{cat}/K_M$  for CAII-catalyzed *p*-nitrophenyl acetate (PNPA) hydrolysis was measured at 25 °C in 50 mM buffer (TAPS (pH 7.6–8.8), MOPS (pH 6.8–7.5), or MES (pH 6.0–6.7)), ionic strength = 0.1 M with sodium sulfate, 0.5 mM PNPA and 0.1–20 μM CAII. The initial rate of ester hydrolysis was monitored at 348 nm ( $\epsilon_{348} = 5000 \text{ M}^{-1} \text{ cm}^{-1}$ ).<sup>35</sup> Background rates were measured in the presence of 0.5 mM acetazolamide. The pK<sub>s</sub>, pH-independent second-order rate constant and standard error were calculated by a weighted fit to eq 3 using Kaleidagraph. However, the data for Q92E CAII were best fit by eq 4, in which an additional constant, A = 24 M<sup>-1</sup> s<sup>-1</sup>, was added. This may reflect ester hydrolysis catalyzed by the zinc-water form of this variant.

$$k_{cat}/K_{M \text{ obs}} = k_{cat}/K_M/(1 + 10^{(pK_a - pH)}) \quad (3)$$

$$k_{cat}/K_{M \text{ obs}} = A + (k_{cat}/K_M/(1 + 10^{(pK_a - pH)})) \quad (4)$$

Initial rates of CO<sub>2</sub> hydration were measured in a KinTek stopped-flow apparatus at 25 °C by the changing pH-indicator method.<sup>16</sup> The reaction was monitored at 578 nm in 50 mM TAPS buffer, pH 8.9, 25 μM *m*-cresol purple, 0.1 mM EDTA, ionic strength = 0.1 M with sodium sulfate, and 0.14–5 μM CAII. The CO<sub>2</sub> concentration varied

(20) Krebs, J. F.; Fierke, C. A.; Ippolito, J. A.; Christianson, D. W. *J. Biol. Chem.* **1993**, *268*, 27458–27466.

(21) Liang, Z.; Xue, Y.; Behravan, G.; Jonsson, B. H.; Lindskog, S. *Eur. J. Biochem.* **1993**, *211*, 821–827.

(22) Xue, Y.; Lijias, A.; Jonsson, B. H.; Lindskog, S. *Proteins: Struct. Funct. Genet.* **1993**, *17*, 93–106.

(23) Kiefer, L. L.; Fierke, C. A. *Biochemistry* **1994**, *33*, 15233–15240.

(24) Ippolito, J. A.; Christianson, D. W. *Biochemistry* **1994**, *33*, 15241–15249.

(25) Coleman, J. E. *J. Biol. Chem.* **1967**, *242*, 5212–5219.

(26) Lindskog, S.; Coleman, J. E. *Proc. Natl. Acad. Sci. U.S.A.* **1973**, *70*, 2505–2508.

(27) Lesburg, C. A.; Christianson, D. W. *J. Am. Chem. Soc.* **1995**, *117*, 6838–6844.

(28) Krebs, J. F.; Fierke, C. A. *J. Biol. Chem.* **1993**, *268*, 948–954.

(29) Sanger, F.; Nicklen, S.; Coulson, A. R. *Proc. Natl. Acad. Sci. U.S.A.* **1977**, *74*, 5463–5467.

(30) Alexander, R. S.; Kiefer, L. L.; Fierke, C. A.; Christianson, D. W. *Biochemistry* **1993**, *32*, 1510–1518.

(31) Osborne, W.; Tashian, R. *Anal. Biochem.* **1975**, *64*, 297–303.

(32) Hunt, J. B.; Rhee, M.; Storm, C. B. *Anal. Biochem.* **1977**, *79*, 614–617.

(33) Hunt, J. B.; Neece, S. H.; Schachman, H. K.; Ginsburg, A. *J. Biol. Chem.* **1984**, *259*, 14793–14803.

(34) Sällén, L. G.; Martell, A. E. *Stability Constants of Metal Ion Complexes, Special Publication No. 17*; The Chemical Society: London, 1964; p 546.

(35) Armstrong, J. M.; Myers, D. V.; Verpoorte, J. A.; Edsall, J. T. *J. Biol. Chem.* **1966**, *241*, 5137–5149.

(36) Khalifah, R. G. *J. Biol. Chem.* **1971**, *246*, 2561–2573.

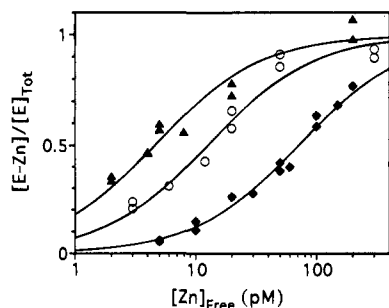


**Figure 2.** Measurement of a zinc dissociation constant for CAII variants at pH 7. The zinc dissociation constant was obtained by dialyzing 0.5 mL of 60  $\mu$ M apo-CAII (either Q92E ( $\blacktriangle$ ), E117D ( $\circ$ ), or T199A ( $\blacklozenge$ ) CAII) for 20 h at 30  $^{\circ}$ C against 1 L of a zinc/dipicolinate buffer (0.0–0.5 mM total zinc/1 mM dipicolinate) in 10 mM Tris sulfate, pH 7. Enzyme bound zinc (E–Zn) was separated from free zinc ( $Zn_{free}$ ) by chromatography on PD-10 columns and then quantitated using a colorimetric PAR assay.<sup>33</sup> The  $[Zn]_{free}$  was calculated from  $[Zn]_{tot}$  as designated in the methods. The data were fit to eq 1 and  $K_D$ 's are listed in Table 1.

**Table 1.** Zinc Dissociation Constants and Dissociation Rate Constants of Wild-Type and CAII Variants<sup>a</sup>

CAII variant	zinc $K_D$ (pM) <sup>b</sup>	zinc $k_{off}$ ( $h^{-1}$ ) <sup>c</sup>	$t_{1/2}$ (day)
wild-type	$4.0 \pm 1^d$	$5.1 \pm 0.3 \times 10^{-3}^e$	$5.2^e$
Q92A	$18 \pm 2$	$1.0 \pm 0.05 \times 10^{-2}$	2.9
Q92L	$30 \pm 8$	$0.12 \pm 0.02$	0.24
Q92N	$5 \pm 1$	$2.6 \pm 0.2 \times 10^{-2}$	1.1
Q92E	$5 \pm 1$	$9.1 \pm 3.0 \times 10^{-4}$	31.7
E117A	$40 \pm 15$	$1.5 \pm 0.3$	0.019
E117D	$12 \pm 2$	$1.1 \pm 0.1$	0.026
Q92A/E117A	$160 \pm 35$	$1.6 \pm 0.6$	0.019
T199A	$60 \pm 10$	$2.1 \pm 0.1 \times 10^{-3}^f$	$14.4^f$

<sup>a</sup> Measured at pH 7.0, 25  $^{\circ}$ C as described in the legends of Figures 2 and 3. <sup>b</sup> Zinc  $K_D$  calculated using eq 1. <sup>c</sup> Zinc  $k_{off}$  calculated using eq 2. <sup>d</sup> Taken from ref 52. <sup>e</sup> Taken from ref 23. <sup>f</sup> C.-C. Huang and C. A. Fierke, unpublished data.

from 3 to 24 mM. Background rates, measured in the absence of CAII, were subtracted from the observed rates.

## Results

To probe the function of second shell hydrogen bonds between residues which ligand zinc (H94, H119, solvent) and amino acid side chains (Q92, E117, and T199, respectively), we constructed a series of CAII variants with alanine at position 92, 117, or 199. In these variants the hydrogen bond acceptor is replaced with either a solvent molecule or another amino acid side chain.<sup>27</sup> In addition, to delineate the essential structural features of these interactions, we changed the charge, size, and hydrophobicity of the amino acid at position 92: Q92 to E, N, and L. The following section describes the metal binding and catalytic properties of these CAII variants.

**Metal Binding.** To assess the effects of altering the indirect ligands on metal binding, we measured a zinc dissociation constant at pH 7 for the CAII variants at positions 92, 117, and 199 using equilibrium dialysis against a zinc/dipicolinate buffer (Figure 2 and Table 1). Substitution of a solvent molecule for the amino acid side chain functioning as a hydrogen bond acceptor for the zinc ligands in the Q92A, T199A, and E117A CAII variants decreases zinc affinity 4.5–15-fold relative to wild-type CAII. Furthermore, this effect is additive since the zinc  $K_D$  of the double substitution variant, Q92A/E117A CAII, is 40-fold larger than wild-type, consistent with the predicted increase based on the loss of zinc affinity for each of the substitutions alone (45-fold). However, zinc avidity is not very sensitive to the structure of the acceptor residue as long as the

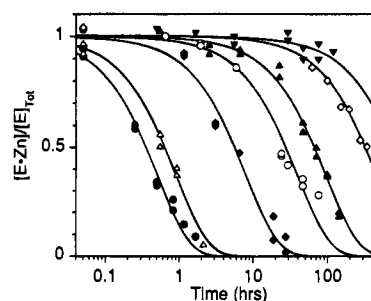


**Figure 3.** Measurement of a zinc dissociation rate constant for CAII variants at pH 7. Measurement of the rate of zinc dissociation was initiated by diluting the CAII variant (either E117A ( $\bullet$ ), E117D ( $\Delta$ ), Q92L ( $\blacklozenge$ ), Q92N ( $\circ$ ), Q92A ( $\blacktriangle$ ), T199A ( $\diamond$ ); or Q92E ( $\blacktriangledown$ ) CAII) into 10 mM Tris sulfate buffer, pH 7, containing EDTA (final concentration 50  $\mu$ M CAII, 35 mM EDTA). At various time intervals enzyme-bound zinc (E–Zn) was separated from EDTA and free zinc ( $Zn_{free}$ ) by chromatography on PD-10 columns and quantitated using the PAR assay.<sup>33</sup> The data were fit to eq 2 and  $k_{off}$ 's are listed in Table 1.

potential for forming a hydrogen bond is maintained; altering the length (Q92N, E117D) or charge (Q92E) of the hydrogen bond acceptor decreases  $K_D \leq 3$ -fold. These data illustrate the importance of each of these interactions for “fine-tuning” zinc affinity. Furthermore, if all four hydrogen bonds are additive, as observed for two of the hydrogen bonds (Q92 and E117), these indirect ligands may increase zinc affinity 10<sup>4</sup>-fold.

Furthermore, to probe the importance of the indirect ligands in determining the long half-time for dissociation of metals from CAII ( $t_{1/2} = 5$  days<sup>23</sup>), we measured the effect of substitutions at positions 92, 117, and 199 in CAII on this half-time. The zinc dissociation rate constants ( $k_{off}$ ) (Figure 3 and Table 1) were determined from the time-dependent disappearance of CAII-bound zinc after dilution into high concentrations of EDTA to trap the dissociated zinc. Unlike dipicolinic acid which efficiently catalyzes the dissociation of zinc from wild-type CAII,<sup>32</sup> EDTA is believed to act only by lowering the free metal ion concentration.<sup>37</sup> Alteration of the hydrogen bond between H94 and Q92 results in relatively modest changes in the dissociation rate constant relative to wild-type CAII;  $k_{off}$  decreases 6-fold for substitution of a negatively charged carboxylate for the carboxamide (Q92E CAII) while for the remaining variants at position 92  $k_{off}$  increases 2- to 24-fold, roughly paralleling the increases in  $K_D$ . Conversely, alteration or removal of the hydrogen bond between H119 and E117 causes significantly larger increases in  $k_{off}$ , up to 300-fold. Furthermore,  $k_{off}$  for the double variant, Q92A/E117A CAII, is increased 310-fold compared to wild-type CAII, very similar to the  $k_{off}$  observed for E117A CAII. Therefore, the indirect ligand to H119 plays an essential role in slow zinc dissociation. These data cannot rule out the possibility that EDTA is catalyzing zinc dissociation in some or all of the CAII variants due to changes in structure or charge. However, this seems unlikely for two reasons: (1) the smallest increases in  $k_{off}$  are observed upon substitution at position 94 which is the most solvent exposed of the three ligands and (2)  $k_{off}$  for E117A CAII is nearly identical to  $k_{off}$  for E117D CAII where the negative charge on the side chain is retained.

The rate constant for zinc association ( $k_{on}$ ) with wild-type CAII can be estimated from the measured zinc  $K_D$  and  $k_{off}$  assuming a single association step where  $k_{on} = k_{off}/K_D (=3.5 \times 10^5 \text{ M}^{-1} \text{ s}^{-1})$ . Under similar experimental conditions, a slightly smaller value for  $k_{on}$  ( $\approx 10^4 \text{ M}^{-1} \text{ s}^{-1}$ ) has been measured

**Table 2.** Steady-State Kinetic Parameters for PNPA Hydrolysis and Zinc–Water  $pK_a^a$ 

CAII variant	$k_{cat}/K_M$ ( $M^{-1} s^{-1}$ ) <sup>b</sup>	$pK_a^b$
wild-type	$2500 \pm 200^c$	$6.8 \pm 0.1^c$
Q92A	$965 \pm 55$	$6.8 \pm 0.1$
Q92L	$1750 \pm 45$	$6.4 \pm 0.1$
Q92N	$675 \pm 45$	$6.9 \pm 0.1$
Q92E	$1362 \pm 110^d$	$7.7 \pm 0.1^d$
E117A	$1325 \pm 120$	$6.9 \pm 0.1$
E117D	$1450 \pm 40$	$6.7 \pm 0.1$
Q92A/E117A	$1540 \pm 40$	$6.8 \pm 0.1$
T199A	$44 \pm 2^e$	$8.3 \pm 0.1^e$

<sup>a</sup> Measured at 25 °C. <sup>b</sup>  $pK_a$  and pH-independent  $k_{cat}/K_M$  calculated using eq 3 and 4. <sup>c</sup> Taken from ref 53. <sup>d</sup> The pH independent  $k_{cat}/K_M$  and  $pK_a$  were calculated using eq 4. <sup>e</sup> Taken from ref 20.

directly for bovine CAII.<sup>38</sup> Similarly,  $k_{on}$  for the CAII variants can be calculated, and as was observed for the zinc dissociation rate constants, the position 92 variants exhibit more moderate changes in  $k_{on}$  (7-fold decrease to 5-fold increase) than the variants at position 117 (30–70-fold increase). These data suggest that a well-formed hydrogen bond between H119 and E117 is a primary determinant of both slow metal ion dissociation and association rate constants.

**Catalysis and  $pK_a$  of Zinc-Bound Solvent.** To delineate the role of indirect ligands on the reactivity and  $pK_a$  of the zinc-bound solvent, we measured the pH dependence of the second-order rate constant for PNPA hydrolysis catalyzed by each of the CAII variants. As observed for wild-type CAII, the pH dependence of PNPA hydrolysis of the variants (except Q92E CAII) is consistent with the ionization of a single enzymic group; the  $pK_a$  and pH-independent rate constants are listed in Table 2. The pH dependence of the esterase activity of wild-type CAII, and likely these variants as well, directly reflects ionization of the zinc–water moiety.<sup>25,26</sup> Alteration of the hydrogen bond between H94 and Q92 or H119 and E117 decreases the pH-independent second-order rate constant for PNPA hydrolysis modestly (1.4- to 4-fold).

The zinc–water  $pK_a$  is also perturbed when the indirect ligands are altered in CAII. The hydrogen bond formed between T199 and zinc–solvent significantly affects the reactivity and ionization of zinc–solvent, as previously described.<sup>20–22</sup> For perturbation of the hydrogen bonds with the His ligands, the most significant changes in the zinc–water  $pK_a$ 's are a 0.4 pH unit decrease and a 0.9 pH unit increase for Q92L and Q92E CAII, respectively. The  $pK_a$  of the zinc–water ligand is indicative of the ability of the zinc to stabilize a negative charge on this ligand, and hence it reflects the effective positive charge on zinc. Therefore, the positive charge on zinc is decreased by the additional negative charge in Q92E CAII and increased by the weakened hydrogen bond in Q92L CAII. These data confirm that the indirect ligands do modulate the reactivity and electrostatic environment of the zinc in CAII. However, the high resolution crystal structures of these variants demonstrate that a hydrogen bond to the zinc ligand is maintained in all cases by recruitment of new hydrogen bond acceptors from the protein or solvent.<sup>27</sup> Consequently, the observed changes in the  $pK_a$  underestimate the magnitude of the effect of the hydrogen bond network on the electrostatic environment of the zinc-bound water.

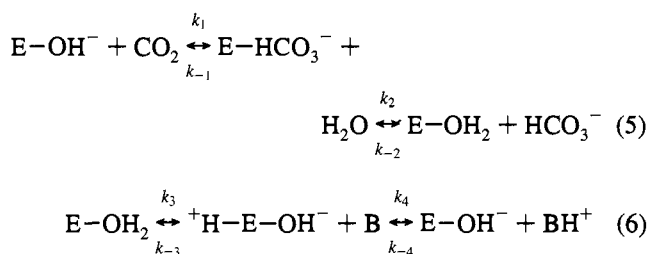
**CO<sub>2</sub> Hydration.** There is considerable evidence that hydration of CO<sub>2</sub> by wild-type CAII consists of two main steps as shown in eqs 5 and 6:<sup>16,39</sup> (1) nucleophilic attack of zinc-bound

**Table 3.** Steady-State Kinetic Parameters of CAII Variants for CO<sub>2</sub> Hydration<sup>a</sup>

CAII variant	$k_{cat}/K_M$ ( $\mu M^{-1} s^{-1}$ )	$k_{cat}$ ( $\times 10^{-5}$ ) ( $s^{-1}$ )	$K_M$ (mM)
wild-type	$110 \pm 10^b$	$10 \pm 1^b$	$8.2 \pm 1.0^b$
Q92A	$29 \pm 0.4$	$4.0 \pm 0.1$	$14 \pm 1.0$
Q92L	$30 \pm 0.8$	$3.7 \pm 0.1$	$12 \pm 1.0$
Q92N	$27 \pm 0.6$	$4.5 \pm 0.1$	$17 \pm 1.0$
Q92E	$12 \pm 2.0$	$2.0 \pm 0.2$	$17 \pm 4.0$
E117A	$19 \pm 0.4$	$4.0 \pm 0.1$	$21 \pm 1.1$
E117D	$27 \pm 0.8$	$3.7 \pm 0.1$	$14 \pm 1.0$
Q92A/E117A	$28 \pm 6.4$	$4.6 \pm 0.4$	$20 \pm 3.0$
T199A	$1.1 \pm 0.05^c$	$0.081 \pm 0.006^c$	$7.4 \pm 1.0^c$

<sup>a</sup> Measured in 50 mM TAPS buffer, pH 8.9, 25  $\mu M$  *m*-cresol purple, 0.1 mM EDTA, ionic strength = 0.1 M with sodium sulfate, 25 °C. <sup>b</sup> Taken from ref 52. <sup>c</sup> Taken from ref 20.

hydroxide on CO<sub>2</sub> to form enzyme-bound HCO<sub>3</sub><sup>−</sup> followed by product dissociation resulting in the zinc–H<sub>2</sub>O form of the enzyme; and (2) proton transfer to solvent via a proton shuttle (H64) to regenerate the zinc–OH<sup>−</sup> species. For wild-type CAII,



$k_{cat}/K_M$  is some combination of the association and CO<sub>2</sub> hydration steps ( $k_{cat}/K_M \approx k_1$  as  $k_2 > k_{-1}$ ). At high CO<sub>2</sub> and buffer concentrations, intramolecular proton transfer between zinc–water and H64 becomes rate-limiting as indicated by a solvent isotope effect of 3–4 on  $k_{cat}$  ( $k_{cat} \approx k_3$  as  $k_4 > k_{-3}$ ).<sup>40</sup> Therefore,  $K_M$  reflects this change in rate-limiting steps, not CO<sub>2</sub> affinity.

The steady-state kinetic parameters for CO<sub>2</sub> hydration, catalyzed by the CAII variants with substitutions in the indirect ligands, were measured at pH 8.9 (Table 3). Altering the hydrogen bond interactions with H94 or H119 uniformly decreases  $k_{cat}/K_M$  for CO<sub>2</sub> hydration by 4–9-fold relative to wild-type CAII, indicating that these indirect ligands stabilize the pentacoordinate transition state for CO<sub>2</sub> hydration relative to the ground state zinc–hydroxide. Similar decreases in  $k_{cat}$  were measured for the CAII variants (2–5-fold), indicating that the rate constant for proton transfer from zinc–water to H64 is likewise moderately decreased by these substitutions. The effect on  $k_{cat}$  does not parallel the  $pK_a$  of the zinc–solvent ligand, as observed for transfer of a proton between an acid and a base in model reactions and between H64 and bases.<sup>41</sup> Therefore, the decreases in  $k_{cat}$  are possibly caused by structural changes in the active site solvent/H64 proton transfer pathway.<sup>19,27</sup> The  $K_M$  values for the variants are increased only slightly ( $\leq 2$ -fold) relative to wild-type CAII. Finally, the effect of perturbing two hydrogen bonds (in Q92A/E117A CAII) on catalysis of CO<sub>2</sub> hydration is not additive.

## Discussion

**Metal Binding.** The indirect ligands in metalloenzymes have been proposed to enhance metal affinity by orienting the ligands for optimal metal coordination and increasing the electrostatic interaction between the ligands and metal ion.<sup>8–10,12</sup> In CAII,

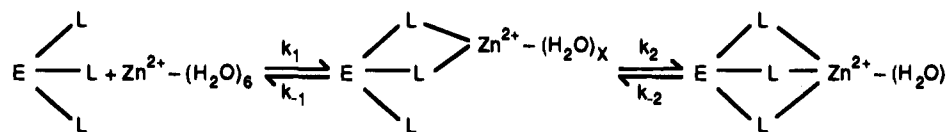
(38) Henkens, R. W.; Sturtevant, J. M. *J. Am. Chem. Soc.* **1968**, *90*, 2669–2676.

(39) Tu, C. K.; Silverman, D. N.; Forsman, C.; Jonsson, B. H.; Lindskog, S. *Biochemistry* **1989**, *28*, 7913–7918.

(40) Steiner, H.; Jonsson, B. H.; Lindskog, S. *Eur. J. Biochem.* **1975**, *59*, 253–259.

(41) Rowlett, R. S.; Silverman, D. N. *J. Am. Chem. Soc.* **1982**, *104*, 6737–6741.

Scheme 1



removal of the side chains that function as hydrogen bond acceptors for the zinc ligands by substitution of A or L for Q92, E117, or T199 decreases zinc affinity by 0.9 to 1.6 kcal/mol at 25 °C ( $\Delta\Delta G = -2.303RT \log(K^{\text{variant}}/K^{\text{wild-type}})$ ). These energetic values are consistent with the values measured by Fersht<sup>42</sup> for loss of a single hydrogen bond to an uncharged donor in an enzyme–substrate complex. However, the high resolution X-ray structures of these CAII variants demonstrate that a hydrogen bond to the zinc ligand is retained.<sup>22,27</sup> In two variants a compensatory hydrogen bond is formed between the histidine zinc ligand and either an inserted water molecule (Q92A CAII) or a chloride ion (E117A CAII).<sup>27</sup> (In our assays that do not contain chloride, it is likely that a water molecule replaces the anion.) However, in other variants structural rearrangements lead to hydrogen bonds with alternative amino acid side chains. In T199A CAII the side chain of E106 is proposed to form a hydrogen bond with the zinc–solvent molecule<sup>22</sup> and in Q92L CAII the side chain of N67 moves to form a poorly oriented hydrogen bond with H94.<sup>27</sup> In all cases the hydrogen bond to the zinc ligand is weakened, due to either the entropic cost of sequestering a solvent molecule into the hydrophobic active site<sup>42</sup> or the nonoptimal hydrogen bonding stereochemistry.

Weakening the hydrogen bonds to the zinc ligands should increase the mobility of the histidine residues in the apo-enzyme and decrease the metal ion affinity due to the increased entropic cost of metal binding. Therefore, the role of indirect zinc ligands is to pre-organize the histidines for optimal metal coordination and avidity.

Furthermore, removing two indirect ligands (Q92 and E117) has an additive effect on zinc affinity, for a decrease in zinc binding of 2.2 kcal/mol. If removal of all four hydrogen bonds has a similar additive effect, the indirect ligands together might increase zinc affinity by as much as 5 kcal/mol. Therefore, these hydrogen bonding interactions may account for a significant fraction of the 8 kcal/mol of increased stability for formation of the CAII–Zn complex compared to interaction between zinc and histidine.<sup>34</sup> These data indicate that the indirect ligands are an essential feature of metalloenzymes conferring avid metal binding and should be included in the construction of novel metal binding proteins. The *de novo* sites with three protein metal ligands bind zinc 10<sup>6</sup>–10<sup>7</sup>-fold less tightly than CAII,<sup>3–6</sup> likely due to a combination of suboptimal arrangement of the direct ligands and absence of second shell hydrogen bonds.

Substitution of Q92 with E was predicted to decrease the zinc  $K_D$  relative to wild-type CAII due to enhanced electrostatic interaction between H94 and zinc in this variant<sup>9</sup> or to a stronger hydrogen bond between E92 and H94 resulting in decreased conformational mobility of the His94 side chain. However, the Q92E CAII variant has metal ion affinity identical to wild-type (Table 1). The X-ray structure of this variant<sup>27</sup> confirms that a favorable hydrogen bond forms between the carboxylate at position 92 and H94 with little perturbation of the active site structure. These data indicate that the charge of the indirect ligand at position 92 is not a primary determinant of metal affinity.

Shortening the length of the side chain functioning as a hydrogen bond acceptor by one methylene group at either

position 92 or 117 might be predicted to weaken the hydrogen bond with the histidine ligand and, therefore, decrease zinc affinity. Substitution of E117 with D decreases zinc affinity by 0.6 kcal/mol relative to wild-type CAII indicating that the hydrogen bond interaction has not been eliminated, but that it is less stable than the equivalent hydrogen bond in wild-type CAII. On the other hand, the zinc  $K_D$  for Q92N is identical to that for wild-type CAII. This is not surprising since the X-ray crystal structure of Q92N CAII<sup>27</sup> reveals that a minor conformational change of the N92 side chain allows the carboxamide to form an optimal hydrogen bond with H94. The decreased steric hindrance and increased solvent accessibility at position 92 relative to position 117 allows for greater flexibility of the amino acid side chain.

**Kinetics of Metal Binding.** The increases in  $k_{\text{off}}$  observed for all of the CAII hydrogen bonding variants, except Q92E, suggest a mechanism of zinc dissociation from CAII in which the rate-limiting step is exchange of the protein metal ligands with solvent.<sup>43</sup> The weakening or removal of the indirect ligands in these CAII variants likely results in increased conformational entropy of the metal ligands, facilitating their exchange with solvent. Indeed, the rate constant for zinc dissociation from CAII decreases with improved geometrical positioning of the ligands for metal coordination in a series of CAII metal ligand variants.<sup>23,24</sup> The decreased zinc  $k_{\text{off}}$  for Q92E relative to wild-type CAII is likely a result of increased electrostatic interaction between H94 and zinc and/or decreased conformational entropy of H94 due to formation of a stronger hydrogen bond with the negatively charged acceptor.<sup>42</sup>

A two-step mechanism for the binding of zinc to wild-type CAII, as well as to some small molecule ligands, is implicated due to the slow association rate constants.<sup>44–47</sup> These data suggest that the rate of formation of many metal complexes is limited by the dissociation of inner-sphere water molecules from the positions to be occupied by the incoming ligands.<sup>44,48</sup> For wild-type CAII, the rate of formation of the protein–zinc complex may be limited by desolvation as suggested for small molecule complexes or, perhaps, by a protein conformational change enabling exchange of the metal ligands. As changing the protein structure should have no effect on  $k_{\text{on}}$  if desolvation is rate-limiting, the changes in  $k_{\text{on}}$  observed for the CAII variants indicate that a rate-limiting protein conformational change is likely.

One possible mechanism for zinc association with wild-type CAII (Scheme 1), proposed to explain the zinc binding properties of a series of CAII metal ligand variants,<sup>23</sup> is also consistent with the metal binding properties of the hydrogen bonding CAII variants. In this model, an initial complex in which zinc is coordinated to two protein ligands occurs prior to formation of the tetrahedral complex containing three protein ligands and a solvent molecule. The rate-limiting step for zinc

(43) Pocker, Y.; Fong, C. T. O. *Biochemistry* **1983**, *22*, 813–818.

(44) Eigen, M. *Proceedings of the 7th International Congress of Coordination Chemistry*; Stockholm, 1962; p 97.

(45) Eigen, M.; Hammes, G. G. *Adv. Enzymol.* **1963**, *25*, 1–38.

(46) Holyer, R. H.; Hubbard, C. D.; Kettle, S. F. A.; Wilkins, R. G. *Inorg. Chem.* **1965**, *4*, 929–935.

(47) Holyer, R. H.; Hubbard, C. D.; Kettle, S. F. A.; Wilkins, R. G. *Inorg. Chem.* **1966**, *5*, 622–625.

(48) Eigen, M.; Wilkins, R. G. *Advances in Chemistry Series, No. 49*; American Chemical Society: Washington, DC, 1965; p 65.

(42) Fersht, A. R. *Trends Biochem. Sci.* **1987**, *12*, 301–304.

association and dissociation is ligand exchange between a solvent molecule and the third protein ligand ( $k_{\text{on}} = k_1 k_2 / k_{-1}$  and  $k_{\text{off}} = k_{-2}$ ). For the position 117 variants, the increased conformational entropy of H119 greatly increases the rate of this exchange such that it is no longer rate-limiting and  $k_{\text{on}}$  approaches the diffusion-control limit ( $k_{\text{on}} = k_1 = 2.5 \times 10^7 \text{ M}^{-1} \text{ s}^{-1}$  for E117D). The large effects on  $k_{\text{on}}$  and  $k_{\text{off}}$  for position 117 relative to position 92 variants may implicate H119 as the last ligand to form in zinc association, and the first to be replaced by solvent during zinc dissociation. Furthermore, the increased rate constant for association in the E117D CAII variant may suggest that the H119 side chain in the wild-type apo-enzyme must reposition for optimal metal coordination.

**Zinc-Water  $pK_a$ .** Christianson and Alexander<sup>9</sup> proposed that carbonyl and carboxylate hydrogen bonding interactions with His zinc ligands may modulate electrostatic interaction between the ligands and zinc. Changes in the electrostatic environment of the zinc in CAII should be reflected by the  $pK_a$  of the zinc-water ligand since this measures the ability of zinc to stabilize a negatively charged hydroxide ion. Analysis of the zinc-water  $pK_a$ 's for the position 117 CAII variants indicates that alterations in the H119/E117 hydrogen bond have little effect on the  $pK_a$ , and by analogy, the effective charge on zinc. However, the effect of deleting the hydrogen bond in E117A CAII may be mitigated by the binding of an anion at this site.<sup>27</sup> On the other hand, substitution of neutral glutamine with negatively charged glutamate at position 92 increases the zinc-water  $pK_a$  by almost one pH unit, probably due to increased electron density on zinc. This indicates that the zinc-hydroxide is destabilized by 1.2 kcal/mol relative to zinc-water compared to wild-type CAII. Furthermore, the zinc-water  $pK_a$  decreases 0.4 units in Q92L CAII where the hydrogen bond to the side chain of N67 is nonoptimal and likely weak.<sup>27</sup> Stabilization of the zinc-bound hydroxide is the predicted effect of removing electron density from zinc. As expected, changes in the indirect ligands have much smaller effects on the electrostatic environment of the zinc than alterations in the direct ligands; substitution of the neutral H94 by negatively charged aspartate or cysteinate destabilizes the zinc-bound hydroxide by  $\geq 4$  kcal/mol. Therefore, the indirect ligands "fine-tune" the electronic environment of the metal in CAII. Similarly, the Asp-His-Fe network in cytochrome *c* peroxidase optimizes the reduction potential and electronic structure of the iron.<sup>15</sup>

**Catalysis.** Any alteration of the hydrogen bond interactions with H94 and/or H119 destabilizes the transition state for  $\text{CO}_2$  hydration relative to wild-type CAII by a minimum of  $\Delta\Delta G^\ddagger = 0.7$  kcal/mol. This decrease in catalytic activity does not appear to correlate with the strength of the hydrogen bond with the histidine ligand nor is the effect additive, therefore it may be related to small structural changes rather than reflecting the electronic environment of the zinc. However, introduction of a negative charge at position 92 decreases stabilization of the transition state for  $\text{CO}_2$  hydration by an additional 0.5 kcal/mol, compared to other amino acids at this position. Although this is a small effect, it is consistent with increased electron density on the zinc ion in this variant destabilizing the negatively-charged transition state for  $\text{CO}_2$  hydration. Indeed, CAII variants with negatively charged direct zinc ligands have significantly reduced catalytic activity ( $10^4$ -fold) for this reason.<sup>23,24</sup>

Alteration of the hydrogen bond with the zinc-solvent in T199A CAII significantly decreases the second-order rate constants for PNPA hydrolysis ( $\Delta\Delta G^\ddagger = 2.4$  kcal/mol) and  $\text{CO}_2$  hydration ( $\Delta\Delta G^\ddagger = 2.7$  kcal/mol).<sup>20,21</sup> However, this hydrogen bond is necessary for the correct positioning of the zinc-

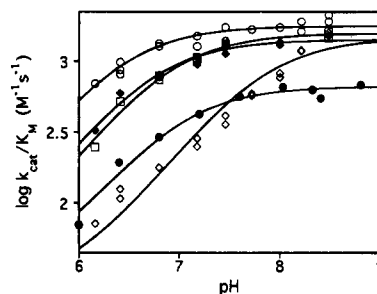


**Figure 4.** pH dependence of  $k_{\text{cat}}/K_M$  for the PNPA esterase activity of Q92L (○), Q92N (●), Q92E (◇), E117D (◆), and Q92A/E117A (□) CAII measured at 25 °C in either 50 mM TAPS (pH 7.8–8.8), 50 mM MOPS (pH 6.8–7.8), or 50 mM MES (pH 6.0–6.8),  $\mu = 0.1$  M with sodium sulfate. The data for all of these variants were fit to eq 3 except Q92E CAII which was fit to eq 4 yielding the values listed in Table 2.

hydroxide for nucleophilic attack on  $\text{CO}_2$  and for direct stabilization of the transition state. Taken together, these data suggest that the main role of the hydrogen bonds with the zinc ligands is to provide tight zinc binding and slow zinc dissociation rather than activate the zinc-bound hydroxide ion, although these interactions do optimize catalytic activity. This result is in contrast to the large decreases in catalytic activity observed for substitution of D650 with E, Q, or A in the zinc protease, neutral endopeptidase 24-11.<sup>14</sup> In this enzyme D650 is believed to hydrogen bond with a His zinc ligand on the basis of amino acid homology with thermolysin. However, the detailed mechanism of this decrease cannot be determined in the absence of the pH dependence of catalysis and structural information. It is likely that D650 has a different or additional role in catalysis in this enzyme.

**Linear Free-Energy Relationships.** A dominant factor controlling nucleophilicity in reactions involving attack of a nucleophile on an amide, ester, or carbonyl carbon is the basic strength of the nucleophile: the stronger the base, the greater the nucleophilicity.<sup>49</sup> Indeed, Brønsted correlations with positive slopes are observed for nucleophilic attack on a carbonyl<sup>50</sup> and hydration of  $\text{CO}_2$  by metal-bound hydroxides in inorganic complexes.<sup>51</sup> Contrary to these results with organic molecules, plots of the pH-independent second-order rate constant ( $\log k_{\text{cat}}/K_M$ ) for PNPA hydrolysis and  $\text{CO}_2$  hydration versus zinc-water  $pK_a$  for the CAII variants show a rough *negative* correlation ( $R = 0.81$ , slope =  $-0.71$ ;  $R = 0.86$ , slope =  $-0.78$ , respectively). A similar result was derived for the esterase and hydrase activity of a series of CAII variants in the metal ligands<sup>23</sup> and at position 199.<sup>20</sup> Furthermore, the parallel effects of these amino acid substitutions on  $\text{CO}_2$  hydration and ester hydrolysis suggest that the rate-limiting step for both catalytic reactions is nucleophilic attack, even in the T199 variants where bicarbonate binding is enhanced.<sup>20–22</sup> A plot of  $\log(k_{\text{cat}}/K_M)$  for  $\text{CO}_2$  hydration versus zinc-water  $pK_a$  for all of these CAII variants is shown in Figure 5. The slope of  $-0.65$  indicates that the interactions which destabilize zinc-hydroxide relative to zinc-water similarly destabilize the negatively charged pentacoordinate transition state for  $\text{CO}_2$  hydration relative to zinc-hydroxide. These data suggest that the negative charge on oxygen in the transition state

(49) Fersht, A. R. *Enzyme Structure and Mechanism*, 2nd ed.; W. H. Freeman & Company: New York, 1985; p 83.

(50) Hudson, R. F.; Klopman, G. *Chemical Reactivity and Reaction Paths*; Wiley: New York, 1974; Chapter 5.

(51) Martin, R. B. *J. Inorg. Nucl. Chem.* **1976**, *38*, 511–513.

(52) Kiefer, L. L.; Krebs, J. F.; Paterno, S. A.; Fierke, C. A. *Biochemistry* **1993**, *32*, 9896–9900.

(53) Fierke, C. A.; Calderone, T. L.; Krebs, J. F. *Biochemistry* **1991**, *30*, 11054–11063.

(54) Alexander, R. S.; Nair, S. K.; Christianson, D. W. *Biochemistry* **1991**, *30*, 11064–11072.

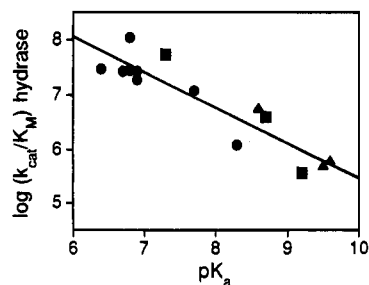


**Figure 5.** Plot of the log of the pH-independent second-order rate constant for CO<sub>2</sub> hydration versus the zinc–water pK<sub>a</sub> for wild-type and variants of CAII, including position 92, position 117, and T199A CAII variants (●); H94C, H94D, and H119D CAII variants<sup>23</sup> (▲); and T199S, T199V, and T199P CAII variants<sup>20</sup> (■). The data are fit to a line yielding  $R = 0.92$ , slope =  $-0.65$ .

retains characteristics of the zinc–hydroxide and that stabilization of this negative charge is the determinant factor in catalysis, rather than the nucleophilicity of the zinc–hydroxide. The

factor most likely destabilizing both zinc–hydroxide and the transition state for the CAII variants is the increased electron density on the zinc ion as a result of (1) replacement of a neutral residue in close proximity to the zinc with a negatively charged residue (position 92 variants), (2) replacement of a neutral metal ligand with a negatively charged ligand,<sup>23</sup> and (3) alteration of the E106/T199/zinc–solvent hydrogen bond network.<sup>20</sup>

**Acknowledgment.** The authors thank Gang Hu, Chih-Chin Huang, and Keith McCall for technical assistance, Dr. Terry Oas for assistance with the molecular graphics, and Charles Lesburg and Dr. David Christianson for helpful discussions. We also thank the National Institutes of Health (GM40602) and the Office of Naval Research (N00014-93-1-1245) for support of this work. Additionally, C.A.F. gratefully acknowledges the receipt of an American Heart Association Established Investigator Award and a David and Lucile Packard Foundation Fellowship in Science and Engineering.

JA9502379